Nanoscale

PAPER

View Article Online
View Journal | View Issue

Cite this: *Nanoscale*, 2018, **10**, 277

Probing magnetic coupling between $LnPc_2$ (Ln = Tb, Er) molecules and the graphene/Ni (111) substrate with and without Au-intercalation: role of the dipolar field†

V. Corradini, *[a] A. Candini,‡[a] D. Klar,[b] R. Biagi,[a,c] V. De Renzi,[a,c] A. Lodi Rizzini,[a,c,d] N. Cavani,[a,c] U. del Pennino,[a,c] S. Klyatskaya,[e] M. Ruben,[e,f] E. Velez-Fort,[g] K. Kummer,[g] N. B. Brookes,[g] P. Gargiani,[h] H. Wende[b] and M. Affronte[a,c]

Lanthanides (Ln) bis-phthalocyanine (Pc), the so-called $LnPc_2$ *double decker*, are a promising class of molecules with a well-defined magnetic anisotropy. In this work, we investigate the magnetic properties of $LnPc_2$ molecules UHV-deposited on a graphene/Ni(111) substrate and how they modify when an Au layer is intercalated between Ni and graphene. X-ray absorption spectroscopy (XAS), and linear and magnetic circular dichroism (XLD and XMCD) were used to characterize the systems and probe the magnetic coupling between $LnPc_2$ molecules and the Ni substrate through graphene, both gold-intercalated and not. Two types of $LnPc_2$ molecules (Ln = Tb, Er) with a different magnetic anisotropy (easy-axis for Tb, easy-plane for Er) were considered. XMCD shows an antiferromagnetic coupling between Ln and Ni(111) even in the presence of the graphene interlayer. Au intercalation causes the vanishing of the interaction between Tb and Ni(111). In contrast, in the case of $ErPc_2$, we found that the gold intercalation does not perturb the magnetic coupling. These results, combined with the magnetic anisotropy of the systems, suggest the possible importance of the magnetic dipolar field contribution for determining the magnetic behaviour.

Received 5th September 2017,
Accepted 15th November 2017

DOI: 10.1039/c7nr06610d

rsc.li/nanoscale

Introduction

Molecules made of a magnetic core and an organic shell are recognized as promising moieties for exploiting magnetism at the nano-scale[1–3] and molecular spintronics. Transition metal porphyrins and phthalocyanines represent a prototypical class of molecules: they can be easily deposited in clean conditions and grow self-assembled ordered layers on metal surfaces.[4] More than a decade ago it was shown that these molecules couple magnetically to ferromagnetic substrates by direct exchange or ligand-mediated superexchange interaction,[5–9] but due to their paramagnetic behaviour they only mimic the substrate magnetization.

Along this line, the class of lanthanides (Ln) bis-phthalocyanine (Pc), the so-called $LnPc_2$ *double decker*, have received considerable attention, since they present the same versatility as the transition metal phthalocyanines and porphyrins, but behave as single molecule magnets (SMMs), retaining their magnetization below a certain blocking temperature.[10,11] This magnetic nature derives from their morphology and electronic configuration: the magnetization of the f-shell Ln ions exhibits a well-defined magnetic anisotropy, as a consequence of the ligand field created by the two Pcs between which the magnetic ions are sandwiched. Furthermore, the neutral derivative $[LnPc_2]^0$ possesses one unpaired electron that is delocalized in the phthalocyanines, making the molecules suitable for ligand-mediated interactions with the substrates.[12]

$TbPc_2$ couples antiferromagnetically when deposited on a magnetic layer and behaves as an independent magnetic unit, given that its magnetization depends critically on the orien-

[a]*Centro S3, Istituto Nanoscienze – CNR, via G. Campi 213/A, 41125 Modena, Italy. E-mail: valdis.corradini@nano.cnr.it*
[b]*Faculty of Physics and Center for Nanointegration Duisburg-Essen (CENIDE), University of Duisburg-Essen, Lotharstraße 1, D-47048 Duisburg, Germany*
[c]*Dipartimento di Scienze Fisiche, Matematiche e Informatiche, Università di Modena e Reggio Emilia, via G. Campi 213/A, 41125 Modena, Italy*
[d]*CNR-IOM, Laboratorio TASC, Area Science Park, S.S. 14, km 163.5, 34012 Basovizza (Trieste), Italy*
[e]*Institute of Nanotechnology, Karlsruhe Institute of Technology (KIT), D-76344 Eggenstein-Leopoldshafen, Germany*
[f]*Institut de Physique et Chimie des Materiaux de Strasbourg, UMR 7504 UdS-CNRS, 67034 Strasbourg Cedex 2, France*
[g]*European Synchrotron Radiation Facility (ESRF), Avenue des Martyrs 71, 38043 Grenoble, France*
[h]*ALBA Synchrotron Light Source, E-08290 Barcelona, Spain*

†Electronic supplementary information (ESI) available. See DOI: 10.1039/c7nr06610d

‡Present address: Istituto di Sintesi Organica e Fotoreattività (ISOF), Consiglio Nazionale delle Ricerche (CNR), Via Gobetti 101, 40129 Bologna, Italy.

tation of the molecule easy axis as well as on the interplay of ligand mediated super-exchange interaction with the substrate and the applied magnetic field.[7] In recent works, we have demonstrated that super-exchange interaction can couple the magnetic moment of the Ln to Ni substrates thanks to a partial overlap of the d-orbitals of the Ln (in turn, mediating the polarization of the inner f-shell electrons) with those of the Pc.[13]

Super-exchange interactions between a magnetic substrate and 3d single atoms/clusters,[14] transition metal phthalocyanines and porphyrins[12,15–17] and $LnPc_2$ SMMs[18] have been observed also when a graphene interlayer is present. In recent years, graphene has been widely studied for applications in the field of spin transport and spintronic devices[19] due to its properties such as high in-plane charge carrier mobility,[20] weak spin–orbit interaction and the capability to passivate metal (and magnetic) surfaces through weak van der Waals interactions with the surface.[21,22] It is therefore extremely interesting to investigate in detail the role of a graphene layer in mediating the coupling between a magnetic substrate and the molecular moieties. We have recently shown, for the case of the $TbPc_2$ molecules, that a graphene layer directly grown on Ni still allows super-exchange coupling through a relay-like mechanism mediated by the electron spin delocalized in the Pc ligands.[18]

In the present work, we pursue this issue, investigating the presence or absence of magnetic coupling between a molecular probe and a graphene/Ni(111) substrate when an Au layer is intercalated between Ni and graphene. In this system, Au acts as a further spacer, increasing the distance between the ferromagnetic substrate and the molecules, and also changes the characteristics of the graphene layer. The most important effect is the decoupling of graphene from the Ni substrate, thus almost restoring its free-standing properties.[23] Moreover, the gold layer induces, through spin–orbit interaction, significant spin splitting of the energy bands of graphene.[24]

For our purposes we focus, as molecular probes, on two $LnPc_2$ derivatives bearing a strong – but different – magnetic anisotropy.[25] $TbPc_2$ has an $L = 3$, $S = 3$, $J = 6$ ground state and the ligand field leads to a huge uniaxial anisotropy, leaving the $m_J = \pm 6$ doublet to behave as an Ising spin with the easy axis perpendicular to the planes of the two phthalocyanines. $ErPc_2$ has an $L = 6$ $S = 3/2$ $J = 15/2$ ground state and the ligand field induces an in-plane anisotropy, leaving the $m_J = \pm 1/2$ as the ground doublet.

After describing the preparation and characterization of the systems, we focus on the results of low temperature XMCD investigations. For the sake of completeness, we compare the molecule behaviour on graphene/Au/Ni with that observed when molecules are deposited directly on bare Ni(111) and on graphene/Ni(111), as reported in previous works.[13,18]

Experimental

The single-layer graphene (SLG) was grown on the Ni(111) single-crystal substrate following the procedure reported in the literature.[26–28] Au intercalation was carried out by evaporating 0.5 nm of gold (monitored by using a quartz microbalance and cross-checked by XPS) on the SLG/Ni(111) surface and subsequently annealing for 10 min at 430 °C as described in ref. 23 and 24. The quality, homogeneity, and cleanliness of both SLG/Ni(111) and SLG/Au/Ni(111) were checked by LEED and by XPS (see Fig. S1†). In particular, after Au intercalation the C 1s shifts from 284.7 eV (strongly interacting graphene) to 284.3 eV (C_{Au}), which corresponds to the non-interacting free-standing graphene. Further proof of the high quality of this interface is the measurement of the graphene π-band dispersion around the K point, performed using Angle-Resolved Photoemission Spectroscopy (ARPES) at the APE beamline of the ELETTRA Synchrotron Radiation Facility[29] and shown in Fig. S2 (see the ESI†). These measurements confirm that the properties of free-standing graphene are restored by the intercalation of a gold layer.

The X-ray Absorption Spectroscopy (XAS) experiments were carried out at the BOREAS beamline[30] of the ALBA Synchrotron Radiation Facility (Spain) and at the ID32 beamline[31] of the European Synchrotron Radiation Facility (ESRF) in Grenoble (France). Once introduced into the experimental chamber, the *ex situ* prepared samples were annealed at 300 °C for 5 min to restore the SLG/Ni(111) and SLG/Au/Ni(111) surfaces. ~0.3 monolayer of $LnPc_2$ molecules (Ln = Tb, Er) was evaporated from well-outgassed powder evaporators, at a temperature of 420 °C and at a base pressure of 1.0×10^{-9} mbar. The evaporation rate and the film thickness were monitored through a calibrated quartz microbalance. The coverage was also cross-checked *in situ* by XAS, using a reference sample with coverage determined by XPS. Furthermore, the chemical integrity and the coverage of the deposited $LnPc_2$ molecules were verified *ex post* by XPS [see ref. 18] and by STM investigations (see the ESI†).

Circularly and linearly polarized XAS measurements at the Ln-$M_{4,5}$ and N-K absorption edges were performed in total electron yield mode. For all measurements, the base pressure in the measurement chamber was 1.0×10^{-10} mbar and the base temperature was 2 K (BOREAS) and 8 K (ID32). XMCD measurements were taken with the photon beam and the external magnetic field B (always collinear) applied either at normal or grazing incidence, *i.e.* at an angle θ equal to 0° and 70°, respectively, relative to the surface normal (Fig. 1d). To avoid beam-induced molecule degradation, we minimized both the power and energy densities, respectively, by defocusing the beam and regularly changing the spot position on the sample. Furthermore, we carefully monitored the XAS spectra lineshape, finding no indication of damage.

The dichroic signal (XMCD) is a measure of the magnetization component along the impinging beam direction of the particular chemical species. It is expressed in percentage, *i.e.* by taking the difference between the two XAS spectra obtained with different X-ray polarizations ($\sigma^{\uparrow\downarrow} - \sigma^{\uparrow\uparrow}$) and dividing it by the edge height of the absorption spectrum obtained by the average of the two polarizations. Note that by defining the value of the dichroic signal in this way, it does not depend on molecular coverage.

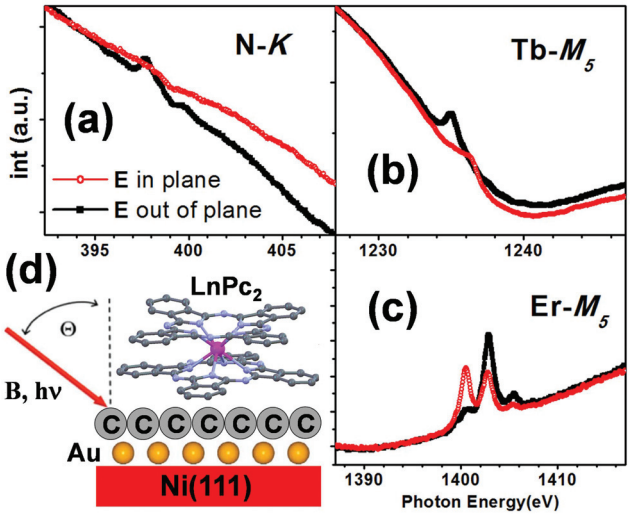

Fig. 1 XLD linearly polarized X-ray absorption spectra at the N-*K* (a), Tb-M_5 (b) and Er-M_5 (c) edges for the $LnPc_2$ on SLG/Au/Ni(111) measured at grazing angle (θ = 70°) at T = 2 K. (d) Sketch of the measuring conditions with the $LnPc_2$ molecule lying flat on the Ni(111)/Au/SLG surface. The magnetic field **B** and the X-ray beam are collinear and oriented at an angle θ = 70° with respect to the normal to the surface. The X-ray linear polarization is chosen to have the electric field either parallel to the sample surface plane or turned 90° from it, *i.e.* lying in the incidence plane.

In this work, we focus our attention on the low magnetic field behaviour of the $LnPc_2$ species: in order to obtain a suitable signal to noise ratio, XMCD data are obtained by integrating over several XAS acquisitions, taken at the two opposite polarizations.

The full-range magnetization curves $M(B)$ (from −5 T to 5 T and the way back), taken for both Ln ions deposited on the bare Ni(111) and on SLG/Au/Ni(111) substrates (Fig. 4 and Fig. S6†), were obtained by plotting the maximum value of the XMCD signal as a function of the external applied magnetic field under isothermal conditions. Measurements in the low-field region [−0.5, 0.5 T] were taken in this specific range after having applied the procedure for minimizing the residual field of the magnet. In order to obtain a satisfactory S/N ratio, for the lowest field values we had to average several tens of spectra for each polarization. This implied a very long time for the acquisition in this field range, allowing us to collect only one way, *i.e.* from −0.5 to 0.5 T. The time required for the whole XMCD measurements in this range was about ten hours.

Conversely, in the case of the SLG/Ni(111) substrate (Fig. 4e and f) and for Ni(111) clean (Fig. 4a and b) Ni magnetization curves were measured in a faster manner, acquiring, for each field, the XAS intensities at the pre-edge (P) and at the energy corresponding to the XMCD maximum (E), and evaluating the quantity:

$$M = [(E\sigma^{\uparrow\downarrow} - P\sigma^{\uparrow\downarrow}) - (E\sigma^{\uparrow\uparrow} - P\sigma^{\uparrow\uparrow})]/1/2[(E\sigma^{\uparrow\downarrow} - P\sigma^{\uparrow\downarrow}) + (E\sigma^{\uparrow\uparrow} - P\sigma^{\uparrow\uparrow})]$$

Results and discussion

System characterization

Linearly polarized X-ray absorption measurements performed at the N-*K*, Tb-M_5 and Er-M_5 edges for the two $LnPc_2$ molecules deposited on SLG/Au/Ni(111) provide us with information on the molecular adsorption geometry. As shown in Fig. 1, the dependence of the spectrum lineshapes on light polarization resembles that of $LnPc_2$ deposited directly on Ni(111) (ref. 13) and on SLG/Ni(111) (ref. 18), proving that, also in this case, the $LnPc_2$ molecules lie flat on the surface, as depicted in panel d.

Typical XAS and X-ray Magnetic Circular Dichroic (XMCD) spectra are shown in Fig. 2 and 3. The lineshape of both XAS and XMCD spectra at the Ln-M_5 edge for the two $LnPc_2$ molecules deposited on SLG/Au/Ni(111) (Fig. 2c) is very similar to that of the corresponding ones obtained with the derivatives deposited on SLG/Ni(111)[18] (Fig. 2b) or directly on Ni(111)[13] (Fig. 2a) and does not change with temperature and magnetic

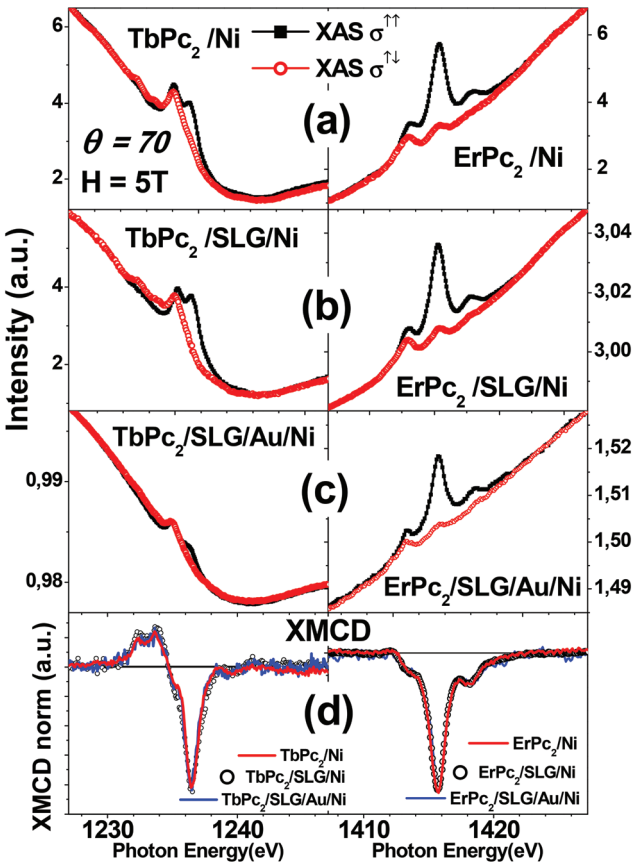

Fig. 2 Comparison of the XAS spectra at the Ln M_5 edge for the $LnPc_2$ on SLG/Au/Ni(111) (panel c) with the corresponding ones obtained on bare Ni(111) (a) and on SLG/Ni(111) (b). The data relative to the $LnPc_2$ molecules deposited on bare Ni(111)[13] and for the $TbPc_2$ on SLG/Ni(111)[18] are taken from our previous works and shown for comparison. The shape of the XMCD spectra (d) is the same for the three substrates. Measurement conditions: H = 5 T, θ = 70°. The temperature is T = 8 K for panels a and b and T = 2 K for panel c.

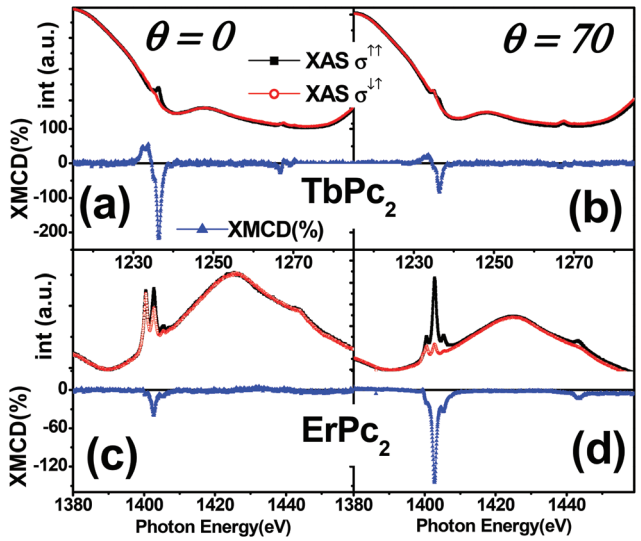

Fig. 3 Absorption spectra taken with $\sigma^{\uparrow\downarrow}$ and $\sigma^{\uparrow\uparrow}$ circularly polarized light (upper spectra in each panel) and the relative XMCD $(\sigma^{\uparrow\downarrow} - \sigma^{\uparrow\uparrow})/(\sigma^{\uparrow\downarrow} + \sigma^{\uparrow\uparrow})/2$ (lower spectra in each panel) at the Ln-$M_{4,5}$ edges for $LnPc_2$ [Tb (a, b), and Er (c, d)] on SLG/Au/Ni(111) at θ = 0° (left panels) and θ = 70° (right panels) incidence angles, taken at an applied external field **B** = 5 T and T = 2 K.

field intensity (Fig. S4†). This allows us to assume the integrity of the adsorbed molecules on all the considered substrates.

XMCD measurements and magnetization curves

As shown in Fig. 3, where the XMCD spectra taken at high field are displayed, the intensity of the dichroic signal strongly depends on the angle θ between the surface and the applied magnetic field. On both SLG/Ni(111) and SLG/Au/Ni(111) substrates, the high-field Tb dichroism is more intense at θ = 0° than at grazing angle (θ = 70°), whilst the opposite occurs for Er, consistent with what was reported in ref. 13 and 18 for the case of bare Ni(111) and SLG/Ni(111) substrates, respectively. This confirms that, for all substrates, the easy axis of the magnetization lies perpendicular to the substrate surface in the case of Tb, whereas it is parallel to the surface plane in the case of erbium.[25]

The different orientation of the molecular easy-axis allowed us to investigate the role of anisotropy in the mechanism determining the molecule–substrate magnetic coupling. To this end, the magnetic coupling between the Ln ions and the Ni substrate was studied by taking the magnetization curves $M(B)$, *i.e.* by measuring the maximum value of the XMCD signal as a function of the external applied magnetic field under isothermal conditions. The full-range magnetization curves (−5 T to 5 T), taken for both Ln ions and for all three possible substrates (*i.e.* bare Ni(111), SLG/Ni(111) and SLG/Au/Ni(111)) are shown in ESI Fig. S6.†

Here, we focus our attention on the low-field region (−1 T, 1 T), where the Zeeman interaction is reduced and the effect of coupling is expected to become predominant. In Fig. 4, the $M(B)$ curves at the Ln-M_5 edge for all three substrates are

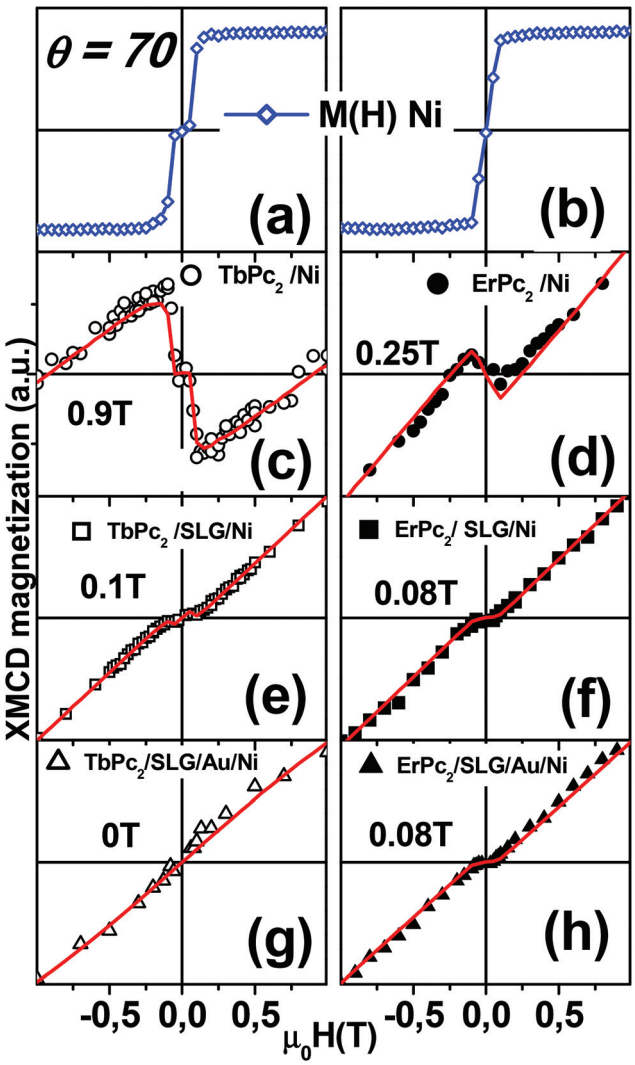

Fig. 4 Comparison of the magnetization curves at the Ni-L_3 (panels a and b) and at the Ln-$M_{4,5}$ edges (Tb: left panels and Er: right panels) at θ = 70°. The hystereses of the two Ni are different because the measurements on $TbPc_2$ and $ErPc_2$ were performed on two different Ni(111) single crystals. The experimental curves (symbols in panels c–h) are in excellent agreement with the simulated ones (red lines) as described in the text. The Ln data are a low-field magnification of Fig. S6.† Data in panels c, d and e are taken from ref. 13 and 18, respectively. In bold we indicate the values of the exchange strength (λ), expressed in Tesla. The temperature is 8 K for all the measurements apart from panel g, measured at T = 2 K.

reported, along with the corresponding simulated curves (see the Discussion). These are compared to the magnetization curves of the corresponding substrates taken at the Ni-L_3 edge: panel (a) reports the $M(B)$ curve measured, at θ = 70°, on the Ni(111) single crystal used for the deposition of the $TbPc_2$ molecule, while the substrate used during the experiments with the $ErPc_2$ molecule is shown in panel (b). The Ni $M(B)$ curves slightly differ from one Ni sample to the other. At variance, we verified that they are not affected by the surface preparation, *i.e.* bare Ni, SLG/Ni or SLG/Au/Ni all show identical $M(B)$ curves.

The Ni and Tb $M(B)$ measured at normal incidence for the $TbPc_2$ deposited on bare Ni, on SLG/Ni(111) and on SLG/Au/Ni(111) are presented in Fig. S5 (see ESI†). We did not show the magnetization for the $ErPc_2$ since the dichroic signal, at $\theta = 0°$, is almost zero.

When the molecules are directly deposited on Ni (panels c and d) we observe that, for small fields, the lanthanide magnetizations are opposite to **B**. On increasing further the field magnitude, a sudden change of the slope sign is observed in correspondence with the field at which the Ni magnetization starts to saturate. Finally, the Ln magnetizations become parallel to the external magnetic field and to the magnetization of the Ni substrate for large enough values of **B**. These features demonstrate the antiferromagnetic character of the coupling of the lanthanide atom to the Ni substrate, in agreement with previously reported findings.[7,13]

When the $LnPc_2$ molecules are deposited on SLG/Ni (panels e and f), although a reversed sign of the magnetization can no longer be measured, a clear change of the slope of the $M(B)$ curves at low fields is still observed. This behaviour shows that, for both molecules, antiferromagnetic coupling with the substrate is still present, although reduced by the presence of the graphene layer. This finding, which has already been reported in the case of $TbPc_2$,[18] is here proved to be valid also in the case of $ErPc_2$.

We now focus our attention on the effects of Au intercalation between graphene and Ni. Extracting reliable XMCD intensity values at very low field, where the dichroic signal is extremely small, is actually not trivial. To this end, we developed a fitting procedure which is illustrated in detail in the ESI.† The results of this analysis are shown in panels g and h of Fig. 4, where the main experimental finding of the present work is reported, *i.e.* the low-field magnetization curves for Tb and Er adsorbed on gold-intercalated SLG. It is observed that, while in the case of $TbPc_2$ the gold intercalation wipes out all kinds of coupling, for $ErPc_2$ the antiferromagnetic coupling between the metal ion magnetic moment and the Ni substrate persists even when they are separated by the gold-intercalated graphene.

Discussion

To obtain a more quantitative estimate of the coupling strength between the magnetic molecules and the underlying Ni substrate in Fig. 4, we superimpose the experimental data with simulated magnetization curves (shown as red lines) of the type $\alpha B_J(B + B_{\mathrm{eff}})$ [ref. 12 and 32], where B_J is the Brillouin function, B is the external magnetic field and α is a coefficient introduced to adjust the simulated curve to the arbitrary XMCD units. B_{eff} is an effective magnetic field, representing the magnetic coupling between the lanthanide atom and the substrate. The origin of this term is usually considered to be a super-exchange type of coupling.[7,13] However, given the tiny energy scales under consideration in this work, we cannot rule out the contribution of the Ni(111) stray field to the observed effective B_{eff} value, as we will explain in more detail in the following.

In all cases, B_{eff} is assumed to be proportional to the Ni magnetization; therefore B_{eff} is defined as $B_{\mathrm{eff}} = \lambda M_{\mathrm{Ni}}$, where M_{Ni} is the Ni(111) magnetization, as measured experimentally by XMCD and normalized to its saturation value, and λ is the parameter related to the strength of the coupling (expressed in Tesla). The curves in Fig. 4 are calculated using $J_{\mathrm{Tb}} = 6$, $J_{\mathrm{Er}} = \frac{1}{2}$, temperature $T = 8$ K and neglecting any anisotropy.

While the correct fit of the full magnetization curves would require the complete theoretical model used in previous works,[7,13,18] for the low magnetic field region which is here of interest, our measured magnetization curves are essentially linear with respect to B and the agreement with the simulated B_J function is already satisfactory. Thus, this simple model allows us to evaluate the strength of the magnetic coupling. In particular, focusing on the $ErPc_2$ behaviour, we found that the estimated strength of the antiferromagnetic coupling is $\lambda = -0.25 \pm 0.02$ T in the case of the bare Ni substrate, $\lambda = -0.08 \pm 0.02$ T in the case of the SLG/Ni substrate and -0.08 ± 0.02 T when $ErPc_2$ molecules are deposited on Au-intercalated SLG on Ni(111).

Instead, in the case of the $TbPc_2$ we found that $\lambda = -0.9 \pm 0.02$ T when $TbPc_2$ molecules are deposited directly on Ni, -0.1 ± 0.02 T on the SLG/Ni substrate and zero for SLG/Au/Ni(111). Here the minus sign accounts for the antiferromagnetic nature of the coupling.

We should here mention that, at variance with measurements performed at grazing incidence ($\theta = 70°$), the TbPc2/SLG/Ni $M(B)$ measurements at $\theta = 0°$ (see the ESI†) does not show any signature of molecule/substrate magnetic coupling. This can be explained considering the angular dependence of the nickel magnetization curves: while at $\theta = 70°$ Ni magnetization saturates already at ~0.2 T, at $\theta = 0°$ saturation occurs only for magnetic field values >0.5 T. Therefore, at $\theta = 0°$ and for fields smaller than 0.5 T, which is the relevant case here, Ni magnetization is significantly smaller than its saturation value, thus substantially hampering the experimental observation of the possible magnetic coupling signature.

The effect of introducing a graphene layer between the molecule and the ferromagnetic Ni(111) substrate has already been discussed in detail in our recent work in the case of $TbPc_2$.[18] Graphene directly grown on Ni still allows magnetic coupling, although a substantial weakening is observed. The intercalation of an Au layer makes the coupling between the Tb magnetic moment and the Ni substrate no more detectable within our experimental accuracy.

The situation is quite different in the case of $ErPc_2$, where the gold intercalation has essentially no effect on the coupling. It is worth remarking here the different relative orientation of the magnetic anisotropy of the two Ln ions (easy-axis for Tb *vs.* easy-plane for Er) and the Ni substrate magnetization. Indeed, the critical role of the alignment between the molecular easy axis and the substrate magnetization has already been demonstrated in the case of $TbPc_2$ on Ni thin films.[7]

Starting from these considerations, we can envisage a qualitative explanation for the observed behaviour, which takes into account the dipolar stray field coming from the magnetization of the nickel substrate. A precise evaluation of the intensity of the substrate-induced stray field would require a detailed knowledge of closure-domain distribution at the surface, which is indeed a demanding issue. Nonetheless, the order of magnitude of the magnetic field intensity at the nickel surface, produced by the uniform magnetization of the whole (macroscopic) crystal, can be estimated calculating the field produced by a uniform collection of magnetic dipoles, each of which is associated with a single atom of the Ni sample (see details of the calculations in the ESI†).

The magnetic field components perpendicular (B_z) and parallel (B_x) to the surface of a disc-shaped sample of radius R and thickness D, calculated along its axis, at a distance d from the surface, are given by:

$$B_x(0,d) = -\frac{\mu_0\mu_B}{4\pi V_{cell}}\sin(\alpha)\left[\frac{-\pi d}{\sqrt{R^2+d^2}}+\frac{\pi(D+d)}{\sqrt{R^2+(D+d)^2}}\right] \xrightarrow{d\ll D} -\frac{\mu_0\mu_B}{4\pi V_{cell}}\sin(\alpha)\left[\frac{\pi D}{\sqrt{R^2+D^2}}\right] \quad (1)$$

$$B_z(0,d) = \frac{\mu_0\mu_B}{4\pi V_{cell}}\cos(\alpha)\left[\frac{-2\pi d}{\sqrt{R^2+d^2}}+\frac{2\pi(D+d)}{\sqrt{R^2+(D+d)^2}}\right] \xrightarrow{d\ll D} \frac{\mu_0\mu_B}{4\pi V_{cell}}\cos(\alpha)\left[\frac{2\pi D}{\sqrt{R^2+D^2}}\right] \quad (2)$$

These results show that the strength of the dipolar field at the surface depends critically on the aspect ratio D/R and is therefore non-negligible in the case (as ours) of macroscopically thick samples. Moreover and most importantly, they demonstrate that the intensity of the dipolar magnetic field does not depend on the distance d from the nickel surface, as long as $d \ll D$ (*i.e.* d is in the nm range, while D is in the mm range).

Upon inserting the values of the Bohr magneton μ_B, the Nickel unit cell volume V_{cell} and the sample dimensions D and R in eqn (1) and (2), we obtain that the magnitude of both components is of the order of tens of mT (B_x = −50 mT and B_z = +35 mT), *i.e.* the same as the coupling strength previously experimentally evaluated.

It is important here to note that the component parallel to the surface is more intense than the orthogonal one. Furthermore, the first is negative, *i.e.* it would provide an antiferromagnetic coupling (with respect to the Ni magnetization) with a magnetic dipole located at the surface, whereas the latter is positive, *i.e.* it would induce a ferromagnetic coupling. The dipolar field felt by the adsorbed molecules is therefore not negligible and essentially the same independently from the layers (SLG, Au) under them. In contrast, the (super-) exchange interaction, being mediated by wave-functions, strongly depends on distance and/or interposed layer. In previous works we proved that SLG was able to keep a significant exchange coupling between Ni and the lanthanide atom. This is true in particular for Tb, which also shows the strongest coupling among the studied lanthanide species. The vanishing of the coupling when gold is intercalated suggests the vanishing of the exchange interaction responsible for the coupling.

So, why does Er keep the same coupling as without gold? Possibly, the coupling of the Er atoms is mainly due to the dipolar field already for the case of the SLG/Ni(111) substrate, and this would come from its in-plane anisotropy, favouring the coupling with the in-plane dipolar field. The invariance of the coupling strength with or without the gold layer is a strong clue in this direction. Of course, a similar interaction is present also for Tb, but the coupling between the in-plane dipolar field and the easy-axis anisotropy, orthogonal to it, makes the coupling too weak to be detected.

In conclusion, we have studied the magnetic coupling between two types of $LnPc_2$ molecules, characterized by different magnetic anisotropies, and a Ni(111) magnetic substrate through an Au-intercalated SLG layer. In the case of Tb, the antiferromagnetic signal – which can be attributed to (super)-exchange coupling, vanishes upon Au intercalation. This effect can be attributed to both the increased distance between the molecular species and the magnetic substrate and to the same mechanisms leading to the intercalation-induced electronic decoupling of the graphene layer from the Ni substrate. A full understanding of the mechanisms underlying the observed vanishing would require a detailed theoretical modelling of the system, which implies considerable computational efforts and is clearly beyond the scope of this work.

In the case of Er on the other hand, the small antiferromagnetic signal does not seem to be affected by intercalation, which can be rationalized by taking into account a relevant contribution of the substrate magnetic dipolar field. Our work therefore suggests the possible importance of the magnetic dipolar field for determining the behaviour of hybrid metal–organic magnetic interfaces, especially when combined with the magnetic anisotropy of the systems.

Conflicts of interest

There are no conflicts to declare.

Acknowledgements

This work was partially supported by the European Community through the FET-Proactive Project MoQuaS by contract no. 610449 and by the Italian Ministry for Research (MIUR) through the PRIN grant 20105ZZTSE "GRAF" and through the Futuro In Ricerca (FIR) grant RBFR13YKWX. We acknowledge the ESRF, ALBA and ELETTRA Synchrotron facilities and their beamline staff for assistance in XAS experiments (beamlines ID32 and BOREAS) and ARPES (APE beamline).

References

1 L. Bogani and W. Wernsdorfer, *Nat. Mater.*, 2008, **7**, 179.
2 S. Sanvito, *Chem. Soc. Rev.*, 2011, **40**, 3336.
3 Y. Lan, S. Klyatskaya, M. Ruben, O. Fuhr, W. Wernsdorfer, A. Candini, V. Corradini, A. Lodi Rizzini, U. del Pennino, F. Troiani, L. Joly, D. Klar, H. Wende and M. Affronte, Magnetic interplay between two different lanthanides in a tris-phthalocyaninato complex: a viable synthetic route and detailed investigation in bulk and on surface, *J. Mater. Chem. C*, 2015, **3**, 9794–9801.
4 A. Cornia, D. Taham and M. Affronte, Thin layers of Molecular Nanomagnets, in *Molecular Magnetic Materials. Concepts and applications*. ed. B. Sieklucka and D. Pinkowicz, Wiley, 2016, ch. 8, pp. 187–230, ISBN: 978-3-527-33953-2.
5 A. Scheybal, T. Ramsvik, R. Bertschinger, M. Putero, F. Nolting and T. A. Jung, *Chem. Phys. Lett.*, 2005, **411**, 214.
6 H. Wende, *et al.*, *Nat. Mater.*, 2007, **6**, 516.
7 A. Lodi Rizzini, *et al.*, *Phys. Rev. Lett.*, 2011, **107**(17), 177205.
8 S. Javaid, M. Bowen, S. Boukari, L. Joly, J.-B. Beaufrand, X. Chen, Y. J. Dappe, F. Scheurer, J.-P. Kappler, J. Arabski, W. Wulfhekel, M. Alouani and E. Beaurepaire, *Phys. Rev. Lett.*, 2010, **105**, 077201.
9 E. Annese, J. Fujii, I. Vobornik, G. Panaccione and G. Rossi, *Phys. Rev. B: Condens. Matter Mater. Phys.*, 2011, **84**, 174443.
10 N. Ishikawa, M. Sugita, T. Ishikawa, S. Koshihara and Y. Kaizu, *J. Am. Chem. Soc.*, 2003, **125**, 8694.
11 N. Ishikawa, M. Sugita, T. Ishikawa, S. Koshihara and Y. Kaizu, *J. Phys. Chem. B*, 2004, **108**, 11265.
12 A. Candini, V. Bellini, D. Klar, V. Corradini, R. Biagi, V. De Renzi, K. Kummer, N. Brooks, U. del Pennino, H. Wende and M. Affronte, Ferromagnetic Exchange Coupling between Fe Phthalocyanine and Ni(111) Surface Mediated by the Extended States of Graphene, *J. Phys. Chem. C*, 2014, **118**, 17670.
13 A. Candini, D. Klar, S. Marocchi, V. Corradini, R. Biagi, V. de Renzi, U. del Pennino, F. Troiani, V. Bellini, S. Klyatskaya, M. Ruben, K. Kummer, N. B. Brookes, H. Huang, A. Soncini, H. Wende and M. Affronte, Spin-communication channels between Ln(III) bis-phthalocyanines molecular nanomagnets and a magnetic substrate, *Sci. Rep.*, 2016, **6**, 21740.
14 A. Barla, *et al.*, *ACS Nano*, 2015, **10**(1), 1101.
15 C. F. Hermanns, *et al.*, *Adv. Mater.*, 2013, **25**(25), 3473.
16 S. Bhandary, O. Eriksson and B. Sanyal, *Sci. Rep.*, 2013, **3**, 3405.
17 D. Klar, S. Bhandary, A. Candini, L. Joly, P. Ohresser, S. Klyatskaya, M. Schleberger, M. Ruben, M. Affronte, O. Eriksson, B. Sanyal and H. Wende, *Phys. Rev. B: Condens. Matter Mater. Phys.*, 2014, **89**, 144411.
18 S. Marocchi, A. Candini, D. Klar, W. Van den Heuvel, H. Huang, F. Troiani, V. Corradini, R. Biagi, V. De Renzi, S. Klyatskaya, K. Kummer, N. B. Brookes, M. Ruben, H. Wende, U. del Pennino, A. Soncini, M. Affronte and V. Bellini, Relay-Like Exchange Mechanism through a Spin Radical between TbPc2 Molecules and Graphene/Ni(111) Substrates, *ACS Nano*, 2016, **10**, 9353–9360.
19 N. Tombros, C. Jozsa, M. Popinciuc, H. T. Jonkman and B. J. van Wees, *Nature*, 2007, **448**(7153), 571.
20 A. K. Geim and K. S. Novoselov, *Nat. Mater.*, 2007, **6**, 183.
21 T. Olsen, J. Yan, J. J. Mortensen and K. S. Thygesen, *Phys. Rev. Lett.*, 2011, **107**, 156401.
22 F. Mittendorfer, A. Garhofer, J. Redinger, J. Klimeš, J. Harl and G. Kresse, *Phys. Rev. B: Condens. Matter Mater. Phys.*, 2011, **84**, 201401(R).
23 A. Varykhalov, J. Sánchez-Barriga, A. M. Shikin, C. Biswas, E. Vescovo, A. Rybkin, D. Marchenko and O. Rader, Electronic and magnetic properties of quasifreestanding graphene on Ni, *Phys. Rev. Lett.*, 2008, **101**, 157601.
24 D. Marchenko, A. Varykhalov, M. R. Scholz, G. Bihlmayer, E. I. Rashba, A. Rybkin, A. M. Shikin and O. Rader, Giant Rashba splitting in graphene due to hybridization with gold, *Nat. Commun.*, 2012, **3**, 1232.
25 N. Ishikawa, M. Sugita and W. Wernsdorfer, Quantum Tunneling of Magnetization in Lanthanide Single-Molecule Magnets: Bis(phthalocyaninato)terbium and Bis(phthalocyaninato)dysprosium Anions, *Angew. Chem., Int. Ed.*, 2005, **44**, 2931.
26 R. Addou, A. Dahal, P. Sutter and M. Batzill, Monolayer graphene growth on Ni(111) by low temperature chemical vapor deposition, *Appl. Phys. Lett.*, 2012, **100**, 021601.
27 J. Lahiri, T. S. Miller, A. J. Ross, L. Adamska, I. I. Oleynik and M. Batzill, Graphene growth and stability at nickel surfaces, *New J. Phys.*, 2011, **13**, 025001.
28 A. Grüneis, K. Kummer and D. V. Vyalikh, Dynamics of graphene growth on a metal surface: a time-dependent photoemission study, *New J. Phys.*, 2009, **11**, 073050.
29 G. Panaccione, *et al.*, *Rev. Sci. Instrum.*, 2009, **80**, 043105.
30 A. Barla, *et al.*, *J. Synchrotron Radiat.*, 2016, **23**, 1507.
31 K. Kummer, *et al.*, *J. Synchrotron Radiat.*, 2016, **23**, 464.
32 C. F. Hermanns, K. Tarafder, M. Bernien, A. Krüger, Y.-M. Chang, P. M. Oppeneer and W. Kuch, Magnetic Coupling of Porphyrin Molecules Through Graphene, *Adv. Mater.*, 2013, **25**, 3473.